

# DISTRIBUTED KALMAN FILTERS FOR RELATIVE FORMATION CONTROL OF MULTI-AGENT SYSTEMS

*Martijn van der Marel and Raj Thilak Rajan*

CAS, Faculty of EEMCS, Delft University of Technology (TUD), The Netherlands

## ABSTRACT

Formation control (FC) of multi-agent systems plays a critical role in a wide variety of fields. In the absence of absolute positioning, agents in FC systems rely on relative position measurements with respect to their neighbors. In distributed filter design literature, relative observation models are comparatively unexplored, and in FC literature, uncertainty models are rarely considered. In this article, we aim to bridge the gap between these domains, by exploring distributed filters tailored for relative FC of swarms. We propose statistically robust data models for tracking relative positions of agents in a FC network, and subsequently propose optimal Kalman filters for both centralized and distributed scenarios. Our simulations highlight the benefits of these estimators, and we identify future research directions based on our proposed framework.

**Index Terms**— Kalman filter, distributed estimation, formation control, relative navigation, multi-agent systems

## 1. INTRODUCTION

Formation control (FC) of multi-agent systems plays a crucial role in various applications, for e.g., in satellite interferometry [1], UAV formation flight [2], and underwater sensing networks [3]. Traditionally, the task of keeping a multi-agent system in the desired formation is performed centrally, however, the inherent distributed nature of multi-agent systems naturally invites a decentralized architecture. One class of distributed methods focus on solving a global optimization problem by distributing the problem over the agents [4], and other solutions are based on behavior-based algorithms [5] or leader-follower architectures [6]. Motivated by the need for FC in GNSS-denied environments (e.g., indoors, in space or underwater), formations in the context of relative navigation have been investigated, where the agents navigate based on their relative dynamics with respect to other mobile agents or objects [7]. One approach to tackle this challenge is through the extension of graph Laplacian-based consensus algorithms [8]. For example, in [9] a multi-agent system with single-integrator dynamics is considered, and closed form solution

for a local control law is proposed, which guarantees the convergence to an affine formation or a rigid formation [10].

A relatively unexplored area within the domain of relative FC is that of statistical uncertainty. In practise, the dynamics of mobile agents and the measurements they make are corrupted by noise, which can be cast as a linear state space model, which motivates the need for designing distributed Kalman filters (KFs). A plethora of existing methods for distributed KFs focus on estimating a common environment state [11, 12], but in case of FC, the agents must track their own dynamical states, which can be seen as subsets of the global state variables. More recently, distributed KFs have been proposed for linear FC systems [13, 14], however, these algorithms require absolute state measurements, which we aim to overcome in this work.

*Notation:* Vectors and matrices are represented by lowercase and uppercase boldface letters respectively.  $A_{ij}$  represents the element on the  $i$ th row and  $j$ th column of the matrix  $\mathbf{A}$ . Sets and graphs are represented using calligraphic letters e.g.,  $\mathcal{A}$ . A vector of length  $N$  of all ones and zeros are denoted by  $\mathbf{1}_N$  and  $\mathbf{0}_N$  respectively. An identity matrix of size  $N$  is denoted by  $\mathbf{I}_N$ . The Kronecker product is  $\otimes$ ,  $\text{tr}(\cdot)$  is the trace,  $\mathbb{E}(\cdot)$  is the expectation, and  $\text{bdiag}(\mathbf{A}_i)_{i \in \mathcal{S}}$  is a block diagonal matrix with blocks  $\mathbf{A}_i \forall i \in \mathcal{S}$ .

### 1.1. Related work

Consider a swarm comprising of  $N$  homogeneous mobile agents moving in  $D$ -dimensional space. The sensing capabilities of the agents are described by the bidirectional sensing graph  $\mathcal{G} = (\mathcal{V}, \mathcal{E})$ , where the nodes of the graph  $\mathcal{V} = \{1, \dots, N\}$  denote the agents. The edges represent the sensing links:  $(i, j) \in \mathcal{E}$  which implies the agent  $i$  can measure its relative position with respect to agent  $j$ . The neighborhood of a node  $i$  is denoted by  $\mathcal{N}_i$ , i.e.  $j \in \mathcal{N}_i$  implies  $(i, j) \in \mathcal{E}$ . The position of agent  $i$  in a  $D$ -dimensional Euclidean space is denoted by the vector  $\mathbf{z}_i \in \mathbb{R}^D$ . We consider the mobile agents to be governed by single-integrator dynamics i.e.,

$$\dot{\mathbf{z}}_i = \mathbf{u}_i \quad (1)$$

$$\mathbf{u}_i = \sum_{j \in \mathcal{N}_i} l_{ij}(\mathbf{z}_i - \mathbf{z}_j) \quad (2)$$

where  $\mathbf{u}_i$  represents the control input of agent  $i$ . Here, the control input for individual agents is a weighted sum of rel-

---

This work is partially funded by the European Leadership Joint Undertaking (ECSEL JU), under grant agreement No 876019, the ADACORSA project - "Airborne Data Collection on Resilient System Architectures."



which concatenate the absolute positions and the control inputs of all agents respectively. The aggregated agent dynamics can then be written as

$$\mathbf{z}_{k+1} = \mathbf{z}_k + \Delta t \mathbf{u}_k + \mathbf{w}_k, \quad \mathbf{w}_k \sim \mathcal{N}(\mathbf{0}_{ND}, \mathbf{Q}) \quad (6)$$

Here, the vector  $\mathbf{w}_k = \{\mathbf{w}_k^i\}_{i=1}^N$  represents the spatial disturbances acting on the agent dynamics, and the covariance matrix  $\mathbf{Q}$  is therefore considered to be a full matrix. Observe that (6) denotes the agent dynamics containing the absolute positions, while the control input is driven by the relative positions w.r.t the neighbouring agents (2). Thus, to map the absolute position vector  $\mathbf{z}_k$  to the relative positions, we exploit the known incidence matrix  $\mathbf{B} = \{B_{il}\}$  of the Graph, whose entries are +1 when  $l$  is directed towards  $i$ , -1 when  $l$  is directed away from  $i$ , and 0 otherwise. Following the convention in [14], the columns of the incidence matrix  $\mathbf{B}$  are grouped per node, starting with all edges directed towards node 1 and ending with edges directed towards node  $N$ . Let  $\mathbf{x}_k = (\mathbf{B}^\top \otimes \mathbf{I}_D) \mathbf{z}_k = \bar{\mathbf{B}}^\top \mathbf{z}_k$  be an edge state vector, the left multiplying (6) by  $\bar{\mathbf{B}}^\top$ , the discrete-time edge dynamics for the entire network is

$$\mathbf{x}_{k+1} = \mathbf{x}_k + \Delta t \bar{\mathbf{B}}^\top \mathbf{u}_k + \bar{\mathbf{w}}_k \quad (7)$$

where  $\bar{\mathbf{w}}_k = \bar{\mathbf{B}}^\top \mathbf{w}_k \sim \mathcal{N}(\mathbf{0}_{ND}, \bar{\mathbf{B}}^\top \mathbf{Q} \bar{\mathbf{B}})$ . Note that for the single-edge dynamical model in (4), the covariance matrix can be retroactively defined as  $\mathbf{Q}_{ij} = \bar{\mathbf{B}}_{ij}^\top \mathbf{Q} \bar{\mathbf{B}}_{ij}$  where  $\bar{\mathbf{B}}_{ij} = \mathbf{b}_{ij} \otimes \mathbf{I}_D$  where  $\mathbf{b}_{ij}$  is the column of the incidence matrix representing the edge  $(i, j)$ . Furthermore, the observation model (3) for the global system is

$$\mathbf{y}_k = \bar{\mathbf{H}} \mathbf{x}_k + \mathbf{v}_k, \quad \mathbf{v}_k \sim \mathcal{N}(\mathbf{0}_{MTD}, \mathbf{R}) \quad (8)$$

with  $\bar{\mathbf{H}} = (\mathbf{I}_M \otimes \mathbf{H})$  where  $M$  is the total number of edges in the network, and  $\mathbf{R} = \text{bdiag}(\mathbf{I}_T \otimes \mathbf{R}_{ij})_{(i,j) \in \mathcal{E}}$  a block diagonal matrix with the ordering of the edges equivalent to that of the incidence matrix. Given (7) and (8), we propose the Centralized Relative Kalman Filter (CRKF) for the entire network as follows.

$$\hat{\mathbf{x}}_{0|0} = \bar{\mathbf{B}}^\top (\mathbf{1}_N \otimes \boldsymbol{\mu}) = \mathbf{0}_{2MD} \quad (9a)$$

$$\boldsymbol{\Sigma}_{0|0} = \bar{\mathbf{B}}^\top (\mathbf{I}_N \otimes \mathbf{P}) \bar{\mathbf{B}} = \mathbf{B}^\top \mathbf{B} \otimes \mathbf{P} \quad (9b)$$

$$\hat{\mathbf{x}}_{k+1|k} = \hat{\mathbf{x}}_{k|k} + \Delta t \bar{\mathbf{B}}^\top \mathbf{u}_k \quad (9c)$$

$$\boldsymbol{\Sigma}_{k+1|k} = \boldsymbol{\Sigma}_{k|k} + \bar{\mathbf{B}}^\top \mathbf{Q} \bar{\mathbf{B}} \quad (9d)$$

$$\mathbf{K}_k = \boldsymbol{\Sigma}_{k|k-1} \bar{\mathbf{H}}^\top (\bar{\mathbf{H}} \boldsymbol{\Sigma}_{k|k-1} \bar{\mathbf{H}}^\top + \mathbf{R})^{-1} \quad (9e)$$

$$\hat{\mathbf{x}}_{k|k} = \hat{\mathbf{x}}_{k|k-1} + \mathbf{K}_k (\mathbf{y}_k - \bar{\mathbf{H}} \hat{\mathbf{x}}_{k|k-1}) \quad (9f)$$

$$\boldsymbol{\Sigma}_{k|k} = (\mathbf{I}_{MD} - \mathbf{K}_k \bar{\mathbf{H}}) \boldsymbol{\Sigma}_{k|k-1} \quad (9g)$$

### 3.2. Joint Relative Kalman filter (JRKF)

To alleviate the centralized collection of information and processing, we propose a distributed algorithm for the CRKF. Observe that the steps in (9) are node separable when the Kalman gain matrix in (9e) is block diagonal i.e., it can be expressed as  $\mathbf{K}_k = \text{bdiag}(\mathbf{K}_k^i)_{i \in \mathcal{V}}$ , where  $\mathbf{K}_k^i \in \mathbb{R}^{M_i D \times M_i T D}$ ,

where  $M_i = |\mathcal{N}_i|$  denotes the cardinality of the neighbourhood of agent  $i$ . However, the key challenge is the distributed computation of the optimal block diagonal Kalman gain matrix.<sup>2</sup> To this end, we propose the following theorem, supported by a lemma.

**Theorem.** *A solution to the Kalman gain  $\mathbf{K}_k^i \in \mathbb{R}^{M_i D \times M_i T D}$  can be computed locally by agent  $i$  by solving the cost function*

$$\min_{\mathbf{K}_k^i, i \in \mathcal{V}} \text{tr}(\boldsymbol{\Sigma}_{k|k}) \quad \text{s.t.} \quad \mathbf{K}_k = \text{bdiag}(\mathbf{K}_k^i)_{i \in \mathcal{V}} \quad (10)$$

which admits the following solution

$$\mathbf{K}_k^i = \boldsymbol{\Sigma}_{k|k-1}^i \mathbf{H}_i^\top \left( \mathbf{H}_i \boldsymbol{\Sigma}_{k|k-1}^i \mathbf{H}_i^\top + \mathbf{R}_i \right)^{-1} \quad (11)$$

where  $\mathbf{H}_i = \mathbf{I}_{M_i} \otimes \mathbf{H}$  and  $\mathbf{R}_i = \text{bdiag}(\mathbf{R}_{ij})_{j \in \mathcal{N}_i}$ .

**Lemma.** *Let  $\mathbf{A} = \text{bdiag}(\mathbf{A}_i)_{i=1}^N$ , and consider  $\mathbf{F}$  with the dimensions of  $\mathbf{A}$ , then  $\text{tr}(\mathbf{A} \mathbf{F} \mathbf{A}^\top) = \sum_{i=1}^N \text{tr}(\mathbf{A}_i \mathbf{F}_{ii} \mathbf{A}_i^\top)$  where  $\{\mathbf{F}_{11}, \mathbf{F}_{22}, \dots, \mathbf{F}_{NN}\}$  are the block diagonal matrices of  $\mathbf{F}$  [18].*

*Proof.* Since minimizing the mean square error in the Kalman updates (9e) is equivalent to minimizing the trace of the posterior covariance, we have (10). Now substituting the Joseph form of the posterior covariance, and introducing  $\boldsymbol{\Phi} = \mathbf{I}_{MD} - \mathbf{K}_k \bar{\mathbf{H}}$ , we have

$$\min_{\mathbf{K}_k^i, i \in \mathcal{V}} \text{tr}(\mathbf{K}_k \mathbf{R} \mathbf{K}_k^\top) + \text{tr}(\boldsymbol{\Phi} \boldsymbol{\Sigma}_{k|k-1} \boldsymbol{\Phi}^\top) \quad (12)$$

s.t.  $\mathbf{K}_k = \text{bdiag}(\mathbf{K}_k^i)_{i \in \mathcal{V}}$

where the constraint guarantees that the Kalman gain matrix  $\mathbf{K}_k$  is block diagonal. Similarly,  $\boldsymbol{\Phi}$  is block diagonal since  $\bar{\mathbf{H}}$  is block diagonal by definition. Now, by introducing  $\boldsymbol{\Phi}_i = \mathbf{I}_{M_i D} - \mathbf{K}_k^i \mathbf{H}_i$  and by applying the Lemma on the second summand of (12), we decouple the optimization problem as

$$\min_{\mathbf{K}_k^i, i \in \mathcal{V}} \text{tr}(\mathbf{K}_k^i \mathbf{R}_i \mathbf{K}_k^{i\top}) + \text{tr}(\boldsymbol{\Phi}_i \boldsymbol{\Sigma}_{k|k-1}^i \boldsymbol{\Phi}_i^\top) \quad (13)$$

Observe that this optimization problem is only minimizing the trace of the local posterior covariance, similar to an unconstrained Kalman gain optimization problem, which has a solution given by (11).  $\square$

In summary, we propose the Joint Relative Kalman Filter

<sup>2</sup>More generally, for any sparsity structure constraint on the Kalman gain matrix, a solution is provided in [14], however this requires a centralized computation.

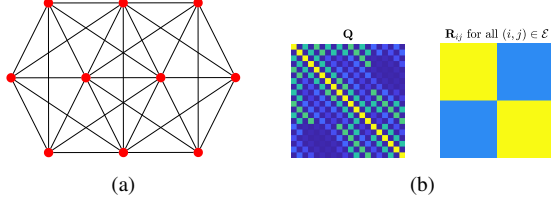


**Fig. 2:** (a) A formation of  $N = 10$  agents with  $M = 60$  bidirectional sensing links in  $D = 2$  dimensions. An illustration of the covariance matrices  $\mathbf{Q}$  and  $\mathbf{R}_{ij}$  used in the simulations.

(JRKF) as follows

$$\hat{\mathbf{x}}_{0|0}^i = \mathbf{0}_{M_i D}, \quad (14a)$$

$$\Sigma_{0|0}^i = \mathbf{B}_i^T \mathbf{B}_i \otimes \mathbf{P} \quad (14b)$$

$$\hat{\mathbf{x}}_{k+1|k}^i = \hat{\mathbf{x}}_{k|k}^i + \Delta t \bar{\mathbf{B}}_i^T \mathbf{u}_k, \quad (14c)$$

$$\Sigma_{k+1|k}^i = \Sigma_{k|k}^i + \bar{\mathbf{B}}_i^T \mathbf{Q} \bar{\mathbf{B}}_i \quad (14d)$$

$$\mathbf{K}_k^i = \Sigma_{k|k-1}^i \mathbf{H}_i^T \left( \mathbf{H}_i \Sigma_{k|k-1}^i \mathbf{H}_i^T + \mathbf{R}_i \right)^{-1} \quad (14e)$$

$$\hat{\mathbf{x}}_k^i = \hat{\mathbf{x}}_{k|k-1}^i + \mathbf{K}_k^i \left( \mathbf{y}_k^i - \mathbf{H}_i \hat{\mathbf{x}}_{k|k-1}^i \right) \quad (14f)$$

$$\Sigma_{k|k}^i = \left( \mathbf{I}_{M_i D} - \mathbf{K}_k^i \mathbf{H}_i \right) \Sigma_{k|k-1}^i \quad (14g)$$

where  $\bar{\mathbf{B}}_i = \mathbf{B}_i \otimes \mathbf{I}_D$  and  $\mathbf{B}_i$  is a submatrix of the incidence matrix  $\mathbf{B}$  containing only the columns representing incoming edges of agent  $i$ . Unlike the RKF, which operates only over a single pairwise relative position, JRKF, jointly estimates the relative positions of multiple neighbours. Finally, note that for both the proposed distributed filters, the prediction steps of agents require the control inputs of neighboring agents, and hence local communication between agents is required.

#### 4. SIMULATIONS

We run simulations to quantify the performance of the proposed filters. We consider a set of mobile agents with single-integrator dynamics (1), following the control law (2). A subset of 3 nodes with an underlying complete subgraph follow the control law in [19] instead, which preserves the inter-agent distances between these leader agents. The formation framework is visualized in Figure 2a. The underlying sensing graph is universally rigid, which guarantees convergence to a rigid formation in the noiseless, continuous-time case as per [9]. Discrete-time simulations should approach this behavior with small time intervals  $\Delta t = 1$  milliseconds. We use the uncertainty model in (6), and the observation model (8) with  $\mathbf{H} = \mathbf{1}_T \otimes \mathbf{I}$  and  $T = 10$ , where the initial positions of agents are drawn i.i.d. from  $\mathcal{N}(\boldsymbol{\mu}, \mathbf{P})$  with  $\boldsymbol{\mu} = \mathbf{0}_D$  and  $\mathbf{P} = \mathbf{I}_D$ . We assume  $\mathbf{Q}$  is constant over time, with diagonal elements  $\sigma_w^2$  and off-diagonal elements in  $[0, \sigma_w^2]$ , and similarly  $\mathbf{R}_{ij}$  are assumed equivalent for all edges  $(i, j)$  with diagonal elements  $\sigma_v^2$  and off-diagonal elements in  $[0, \sigma_v^2]$ . See Figure 2b.

To illustrate the performance of the proposed algorithms, the paths of individual agents and their final positions for a

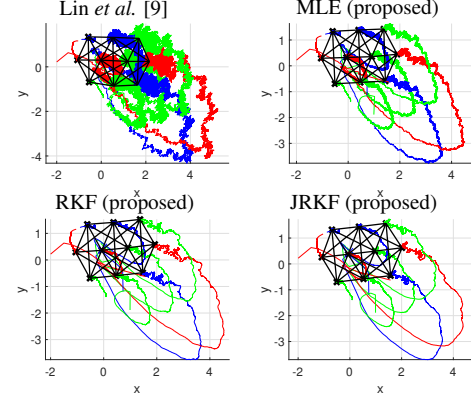


**Fig. 3:** Paths of agents in  $\mathbb{R}^2$  over time for the proposed estimators

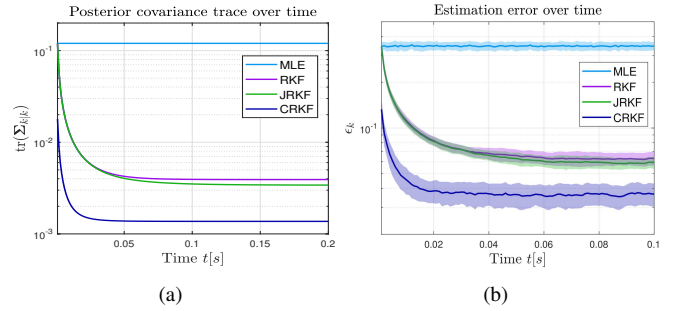


**Fig. 4:** (a) Trace of the posterior covariance over time ( $\sigma_w = 0.001, \sigma_v = 0.1$ ) for the proposed estimators. (b) Estimation error over time ( $\sigma_w = 0.001, \sigma_v = 0.1$ ) for the proposed estimators, where the mean and  $\pm 1\sigma$  regions of the estimation errors are plotted.

single run of the simulation are shown in Figure 3. We use [9] as the benchmark for the performance of the proposed algorithms. The proposed MLE and Kalman filters converge to similar formations, however the traversed paths of agents of the proposed Kalman filters are smoother compared to prevalent methods. Figure 4a shows the evolution of the posterior covariance trace over time, while the agents converge to rigid formations from their initial positions. Here, the uncertainty in edge state estimates remains constant over time for the MLE, whereas the Kalman filters use the past measurements effectively to improve estimates over time. The steady state posterior covariance trace is lowest for the CRKF, and JRKF shows an improvement over the RKF in steady state.

Furthermore, Monte Carlo simulations were performed, where for each run, the estimation error  $\epsilon_k = \|\mathbf{x}_k - \hat{\mathbf{x}}_{k|k}\|_2$  is computed, which is the Euclidean norm of the edge estimation error at time step  $k$ . In Figure 4b, the mean estimation error over 50 runs is shown, along with the  $\pm 1\sigma$  regions. The CRKF shows the best performance in terms of estimation error, which is expected since it is the optimal filter for the global system. Among the two proposed distributed filters, the JRKF shows significant improvement over the single-edge RKF in steady-state estimation error. Observe that in the absence of external disturbances, the edge state-space mod-

els decouple and the joint filter performs equivalently to the single-edge filter.

## 5. SUMMARY

In this paper, we proposed a statistically robust framework for estimating relative positions of agents in a FC system. In addition to the closed form MLE, and an optimal centralized Kalman filter (CRKF), we proposed two distributed Kalman filters for both local and global state-space models. Among the proposed filters in this work, the joint Kalman filter (JRKF) is derived as the optimal filter under the sensing graph constraints for the given model. To let the disturbance model better reflect real-world systems, spatio-temporal disturbance correlation may be introduced, which naturally leads to the kriged Kalman filters.

## 6. REFERENCES

- [1] Guo Ping Liu and Shijie Zhang, "A Survey on Formation Control of Small Satellites," *Proceedings of the IEEE*, vol. 106, no. 3, pp. 440–457, April 2018.
- [2] Yao Zou, Zeqiang Zhou, Xiwang Dong, and Ziyang Meng, "Distributed Formation Control for Multiple Vertical Takeoff and Landing UAVs with Switching Topologies," *IEEE/ASME Transactions on Mechatronics*, vol. 23, no. 4, pp. 1750–1761, August 2018.
- [3] Charalampos P. Bechlioulis, Fotis Giagkas, George C. Karras, and Kostas J. Kyriakopoulos, "Robust Formation Control for Multiple Underwater Vehicles," *Frontiers in Robotics and AI*, vol. 6, pp. 90, September 2019.
- [4] R.L. Raffard, C.J. Tomlin, and S.P. Boyd, "Distributed optimization for cooperative agents: application to formation flight," in *2004 43rd IEEE Conference on Decision and Control (CDC)*, 2004, pp. 2453–2459.
- [5] Tucker Balch and Ronald C. Arkin, "Behavior-based formation control for multirobot teams," *IEEE Transactions on Robotics and Automation*, vol. 14, no. 6, pp. 926–939, 1998.
- [6] Fei Chen and Dimos V. Dimarogonas, "Leader-follower formation control with prescribed performance guarantees," *IEEE Transactions on Control of Network Systems*, vol. 8, no. 1, pp. 450–461, March 2021.
- [7] Cheng Hui, Chen Yousheng, and Wong Wing Shing, "Trajectory tracking and formation flight of autonomous uavs in GPS-denied environments using onboard sensing," in *Proceedings of 2014 IEEE Chinese Guidance, Navigation and Control Conference*, 2014, pp. 2639–2645.
- [8] Zhi-min Han, Zhi-yun Lin, Min-yue Fu, and Zhi-yong Chen, "Distributed coordination in multi-agent systems: a graph laplacian perspective," *Frontiers of Information Technology & Electronic Engineering*, vol. 16, no. 6, pp. 429–448, 2015.
- [9] Zhiyun Lin, Lili Wang, Zhiyong Chen, Minyue Fu, and Zhimin Han, "Necessary and sufficient graphical conditions for affine formation control," *IEEE Transactions on Automatic Control*, vol. 61, no. 10, pp. 2877–2891, 2016.
- [10] Myoung Chul Park, Zhiyong Sun, Brian D.O. Anderson, and Hyo Sung Ahn, "Distance-based control of Kn formations in general space with almost global convergence," *IEEE Transactions on Automatic Control*, vol. 63, no. 8, pp. 2678–2685, August 2018.
- [11] Reza Olfati-Saber, "Distributed kalman filter with embedded consensus filters," *Proceedings of the 44th IEEE Conference on Decision and Control*, pp. 8179–8184, 2005.
- [12] Sayed Pouria Talebi and Stefan Werner, "Distributed kalman filtering and control through embedded average consensus information fusion," *IEEE Transactions on Automatic Control*, vol. 64, pp. 4396–4403, 2019.
- [13] Damián Marelli, Mohsen Zamani, Minyue Fu, and Brett Ninness, "Distributed Kalman filter in a network of linear systems," *Systems and Control Letters*, vol. 116, pp. 71–77, June 2018.
- [14] Daniel Viegas, Pedro Batista, Paulo Oliveira, and Carlos Silvestre, "Discrete-time distributed Kalman filter design for formations of autonomous vehicles," *Control Engineering Practice*, vol. 75, pp. 55–68, June 2018.
- [15] R Michael Buehrer, Henk Wymeersch, and Reza Monir Vaghefi, "Collaborative sensor network localization: Algorithms and practical issues," *Proceedings of the IEEE*, vol. 106, no. 6, pp. 1089–1114, 2018.
- [16] Raj Thilak Rajan, Geert Leus, and Alle-Jan van der Veen, "Relative kinematics of an anchorless network," *Signal Processing*, vol. 157, pp. 266–279, 2019.
- [17] Shunyi Zhao and Biao Huang, "On initialization of the Kalman filter," *2017 6th International Symposium on Advanced Control of Industrial Processes, AdCONIP 2017*, pp. 565–570, 7 2017.
- [18] Gene Howard Golub and Van Loan Charles F., *Matrix computations*, John Hopkins University Press, 1996.
- [19] Dimos V. Dimarogonas and Karl H. Johansson, "Further results on the stability of distance-based multi-robot formations," in *Proceedings of the American Control Conference*, 2009, pp. 2972–2977.